VOL. 10, NO 21, NOVEMBER, 2015 ISSN 1819-6608
ARPN Journal of Engineering and Applied Sciences

www.arpnjournals.com

EXPERIMENTAL VERIFICATION OF MULTILEVEL INVERTER WITH MPPT BASED SOLAR ENERGY

Ramani Kannan[1], S. Shanmuga Priyan[2] and Joga Dharma Setiawan[3]
[1]Department of Electrical and Electronics Engineering, Universiti Teknologi Petronas, Bandar Seri Iskandar, Perak, Malaysia
[2]Department of Electrical and Electronics Engineering, Dhirajlal Gandhi College of Technology, Salem, Tamilnadu, India
[3]Department of Mechanical Engineering, Universiti Teknologi Petronas, Bandar Seri Iskandar, Perak, Malaysia
E-Mail: kreee82@gmail.com

ABSTRACT

This paper concentrates on the implementation of seven level flying capacitor multilevel inverter (FCMLI), focusing on the reduction of total harmonic distortion (THD) in a proposed type of inverter with the help of closed loop control scheme. Among the various types of multilevel inverter (MLI) topologies, FCMLI provides more advantages. The development of closed loop model for seven level FCMLI dramatically reduces the low-order harmonics and THD. Extensive simulation has been applied to compare the performance of the proposed system in closed loop control scheme with that of the open loop control scheme. In order to justify the merits of the proposed system, it is interfaced with the single phase lamp load and analyzed through simulation. This research paper is based on the approach that by tracking the load terminal voltage as the feedback thereby the closed loop scheme is designed. A prototype model for the proposed system is implemented with the single phase induction motor load whose switching is done by using ATmega16 Microcontroller and analyzed the system through hardware results.

Keywords: THD, multi-level inverter, soalr energy, FCMLI.

INTRODUCTION

With the increasing concern about the non-renewable energy sources, constant increase in the prices of fossil fuels, global warming and damage to environment and ecosystem, the renewable energy is becoming more popular and is gaining more attention as an alternative to non-renewable energy sources [1-2]. In recent years, there has been an increasing interest in electrical power generation from renewable-energy sources, such as photovoltaic (PV) or wind-power systems [3-4].

The benefits of power generation from these sources are widely accepted. They are essentially inexhaustible and environmentally friendly. Among the different renewable-energy sources possible to obtain electricity, solar energy has been one of the most active research areas in the past decades, both for grid connected and stand-alone applications [5-6].

The power delivered by a PV system of one or more photovoltaic cells is dependent on the irradiance, temperature, and the current drawn from the cells. Maximum Power Point Tracking (MPPT) is used to obtain the maximum power from these systems. Such applications as putting power on the grid, charging batteries, or powering an electric motor benefit from MPPT. In these applications, the load can demand more power than the PV system can deliver. In this case, a power conversion system is used to maximize the power from the PV system.

There are many different approaches to maximizing the power from a PV system, these ranges from using simple voltage relationships to more complex multiple sample based analysis. Depending on the end application and the dynamics of the irradiance, the power conversion engineer needs to evaluate the various options [7].

The direct current (DC) electrical energy of PV module can be converted to AC electrical energy using inverter [8-11]. Multilevel power converters have become increasingly popular in recent years due to their high-power, high voltage capacity, low switching losses and low electromagnetic concerns [12-13]. Nowadays different topologies have been reported for multi-level inverters [14-17]. They are named as neutral point clamped (diode-clamped) inverter, flying capacitor (capacitor-clamped) inverter and cascaded multi-cell (cascaded H-Bridge) with separated DC source inverter [18-21].

In this paper, Proportional-Integral-Derivative (PID) controllers based closed loop system for seven levels FCMLI and for capacitor clamped DC/DC boost converter have been developed. This scheme maintains the output voltage stability, reducing the harmonic content in the output there by improving the overall system performance. Through the proposed system, THD can be significantly reduced which is confirmed through simulation investigation.

The main contribution of this paper is based on the design and development of prototype model for the proposed system which includes various units such as PV unit, boost converter unit, FCMLI unit, controller unit and display unit.

FCMLI with closed loop control scheme

For this proposed topology, DC input to the system is a solar energy which is harvested from the Sun based on the irradiation and insolation level. In this system a single stand-alone PV module of 12V capacity is used to obtain the DC voltage. Then, this obtained DC voltage is given as the input to the Capacitor Clamped DC/DC Boost Converter. By the DC/DC boost converter topology, the 12V DC is boosted-up into 48V DC. It is illustrated in Figure-1.

In order to maintain the constant DC voltage from the boost converter, a closed loop block is designed in which the actual DC voltage is compared with the 48V DC set value. Based on the error signal from the comparator, the PID controller produces the control signal to the PWM pulse generator block. Then, based upon the specified switching frequency of MOSFET; switching pulses are given to the single switch in the proposed DC/DC boost converter. Then the boosted DC voltage is given as the input to the seven level FCMLI which is intended for 48V DC to 48V AC conversion.

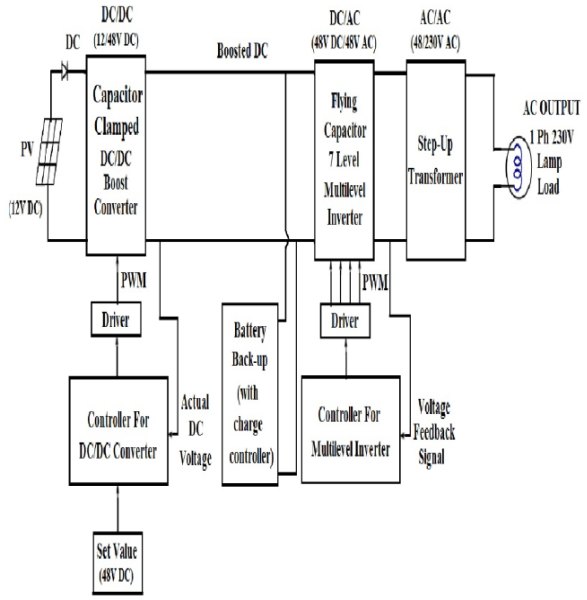

Figure-1. Block diagram of FCMLI with closed loop control scheme.

For controlling the FCMLI, a closed loop block is designed which consists of voltage measurement, voltage controller - PID controller and Sin generator block. With the help of these blocks, a closed loop design is achieved for proposed FCMLI. Then, this low voltage AC signal of 48V AC is given to the step-up transformer for stepping up the voltage level to 230V AC. Finally, a resistive load - single phase lamp load is connected across the 230V AC output terminals. In order to feed the load continuously without any interruption, a battery back-up with charge controller unit is used in-between the DC/DC boost converter and FCMLI blocks.

Photovoltaic system

PV technology has developed rapidly over the last two decades from a small scale, specialist industry supplying the United States space program to a broadly based global activity. Solar panel is the fundamental energy conversion component of PV systems. Its conversion efficiency depends on many extrinsic factors, such as insolation (incident solar radiation) levels, temperature, and load condition.

PV is the direct conversion of light into electricity at the atomic level. Some materials exhibit a property known as the photoelectric effect that causes them to absorb photons of light and release electrons. When these free electrons are captured, electric current results that can be used as electricity. For solar cells, a thin semiconductor wafer is specially treated to form an electric field, positive on one side and negative on the other. When light energy strikes the solar cell, it produces an electric power which can be fed to the desired load. Table-1 shows the technical specifications.

Table-1. Technical specifications of a PV panel.

Parameters	Specifications	Units
Short Circuit Current (I_{sc})	5.45A	Amperes
Open Circuit Voltage (V_{oc})	12V	Voltage
Current at P_{max}	4.95A	Amperes
Voltage at P_{max}	17.2V	Voltage
Insolation	1000 W/m^2 (Constant)	Watts / metre^2

Capacitor clamped DC/DC boost converter

High-Power DC/DC converters are a crucial component of today's emerging vehicular technologies, such as hybrid-electric, battery-electric, and fuel-cell vehicles. Typically, a voltage boost is required to step up the low voltage of the fuel cell or battery to the required high voltage levels. In these applications, it is imperative that the size and mass of the converter are reduced to facilitate packaging due to higher power density. Furthermore, the converter should feature a simple design with high-efficiency operation over the entire load range. In recent years, a number of circuits and control techniques have been proposed to reduce the switching losses in DC/DC boost converters [7].

Configuration of capacitor clamped DC/DC boost converter

With this circuit topology, a low voltage DC from PV panel is boosted-up to the required level in a single stage since it employs a single MOSFET as the switching device. Due to this, the switching and conduction losses are reduced to the great extent. It is illustrated in Figure-2.

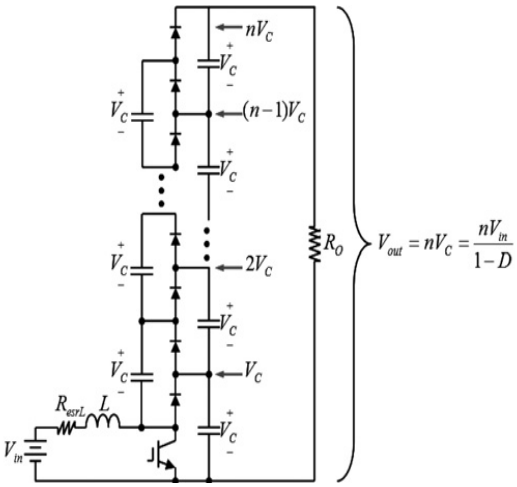

Figure-2. Basic configuration of capacitor clamped DC/DC boost converter for Nx or N+1 levels.

The proposed circuit is based on the multilevel converter principle, where each device blocks only one voltage level achieving high-voltage converters with low-voltage devices. It is a NxDC/DC converter based on one driven switch, 2N+1diodes and 2N+1 capacitors.

One advantage of this topology is that the number of levels can be extended by only adding capacitors and diodes and the main circuit does not need to be modified.

Flying capacitor multilevel inverter

MLI is based on the fact that sine wave can be approximated to a stepped waveform having large number of steps. The steps being supplied from different DC levels supported by series connected batteries or capacitors. The unique structure of MLI allows them to reach high voltages and therefore lower voltage rating device can be used. As the number of levels increases, the synthesized output waveform has more steps, producing a very fine stair case wave and approaching very closely to the desired sine wave.

It can be easily understood that as motor steps are included in the waveform the harmonic distortion of the output wave decrease, approaching zero as the number of levels approaches infinity. Hence, MLI's inverters offer a better choice at the high power end because the high volt-ampere ratings are possible with these inverters without the problems of high dv/dt and the other associated ones [8].

Configuration of seven level FCMLI

The FCMLI requires a large number of capacitors to clamp the device (switch) voltage to one capacitor voltage level. Provided all the capacitors are of equal value, The size of the voltage increment between two consecutive legs of the clamping capacitors defines the size of voltage steps in the output waveform, if the voltage of the main DC-link capacitor is V_{dc} the voltage of the innermost capacitor clamping the innermost two devices is $V_{dc}/(n-1)$.The voltage of the next innermost capacitor will be $V_{dc}/(n-1) + V_{dc}/(n-1) = 2\ V_{dc}/(n-1)$ and so on.

Each next clamping capacitor will have the voltage increment of $V_{dc}/(n-1)$ from its immediate inner one. The voltage levels and the arrangements of the flying capacitors in the FCMLI structure assures that the voltage stress across each main device is same and is equal to $V_{dc}/(n-1)$ for an n- level inverter. Figure-3 illustrates a one phase leg of seven-level FCMLI.

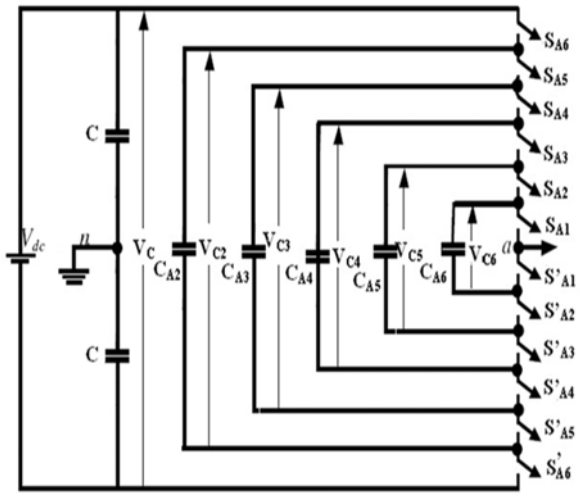

Figure-3. One phase leg of a seven level FCMLI.

For a three phase inverter, two more legs of same construction are coupled to the same DC-link battery V_{dc}. In the Figure-3 shows each switch S_{A1} to S_{A6} and S'_{A1} to S'_{A6} consists of a power semiconductor device (e.g. GTO, IGBT) and an anti-parallel diode. Voltages V_C, V_{c2}, V_{c3}, V_{c4}, V_{c5}, and V_{c6} are V_{dc}, 5/6 V_{dc}, 2/3 V_{dc}, $V_{dc}/2$, $V_{dc}/3$, and $V_{dc}/6$ respectively, as n = 7.

Component count comparison of multilevel inverters

Table-2 summarizes the required number of switches, their gate drivers, clamping diodes, and capacitors of the three types of multilevel inverters for a given number of output voltage levels m.

Table-2. Component count comparison of multilevel inverters.

Components used	Cascaded H-bridge	Diode-clamped	Flying-capacitor
Switches	2x(m-1)	2x(m-1)	2x(m-1)
Gate drivers	2x(m-1)	2x(m-1)	2x(m-1)
Clamping Diodes	-	2x(m-2)	-
Clamping Capacitors	-	-	m-2
Voltage Splitting Capacitors	-	m-1	-

SIMULATION RESULTS AND DISCUSSIONS

The Simulated output is taken for 1000 watts/m^2 of Insolation and 25^{o}C of Temperature under STC. The corresponding DC output voltage waveformof a PV panel is shown in Figure-4.

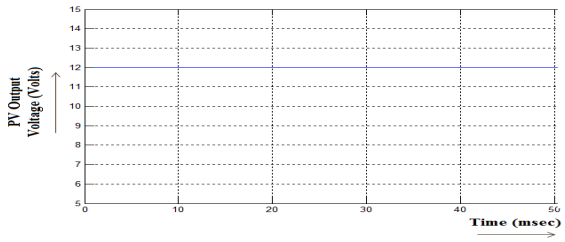

Figure-4. DC output voltage waveform of a PV panel.

Thus from the PV Panel, a 12V DC of Unidirectional Voltage is produced as indicated by blue line in Figure-4. Then this low value of DC voltage is given to the Boost converter for achieving desired voltage for giving input to the Multilevel Inverter.

The Simulated output of Boost Converter is taken based on the various parameter values which are used in the Boost Converter model. Figures-5 shows the DC output voltage waveform of a capacitor clamped DC/DC boost converter.

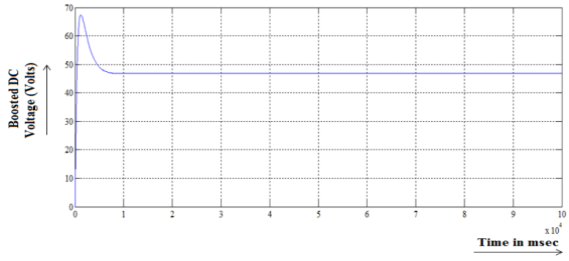

Figure-5. DC output voltage waveform capacitor clamped DC/DC boost converter.

From the PV panel a 12V DC voltage is obtained. This unidirectional DC voltage is then given to the Capacitor Clamped DC/DC Boost Converter for boosting up the voltage up to 48V DC as indicated by blue line in Figure-5.

Figure-6 shows the generic PDPWM method for gate pulse generation.

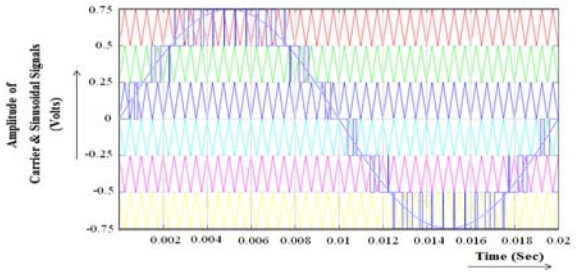

Figure-6. Generic PDPWM method for gate pulse generation.

It illustrates the comparison of six numbers of carrier signals and the sinusoidal modulating signal, in which the sinusoidal signal is superimposed over the carrier signals for generating appropriate PWM pulses.

The Simulation is taken for the Seven Level FCMLI with Multicarrier Pulse Width Modulation Technique. The corresponding AC output voltage waveform of open loop seven level FCMLI system is shown in Figure-7.

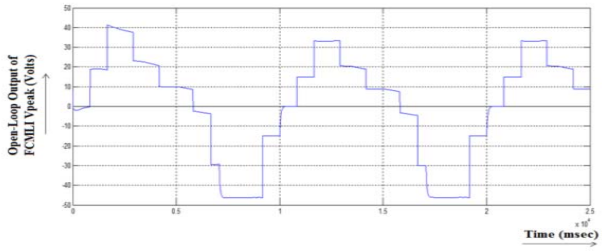

Figure-7. AC output voltage waveform of open loop seven level FCMLI system.

The result of THD analysis performed for open-loop seven level FCMLI system is shown in Figure-8.

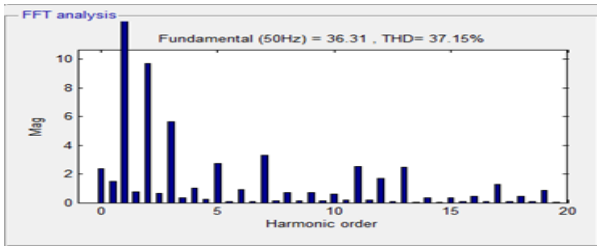

Figure-8. FFT analysis of open loop seven level FCMLI system.

Figures 9 and 10 show the AC output voltage waveform and FFT spectrum of closed loop seven level FCMLI system.

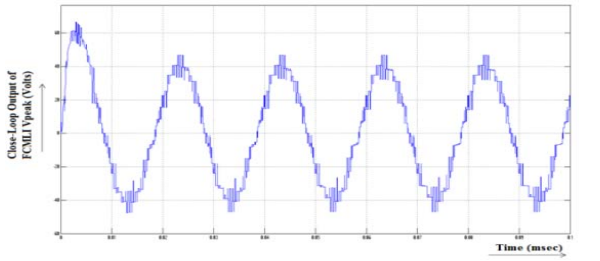

Figure-9. AC output voltage waveform of closed loop seven level FCMLI system.

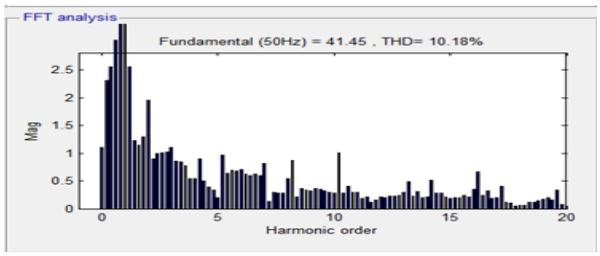

Figure-10. FFT analysis of closed loop seven level FCMLI system.

Therefore in order to reduce the THD level of multilevel inverter output and to improve the performance of the system, a closed-loop design is essential for multilevel inverter. By implementing the closed-loop system, the THD level can be reduced to certain extend. It is clear that the AC output voltage waveform of closed loop model is nearly sinusoidal with more precise steps.

Figure-11 shows the AC load voltage waveform of the proposed closed loop seven level FCMLI system which is measured across the (48/230V AC) step-up transformer. This AC voltage is fed to the single phase lamp load.

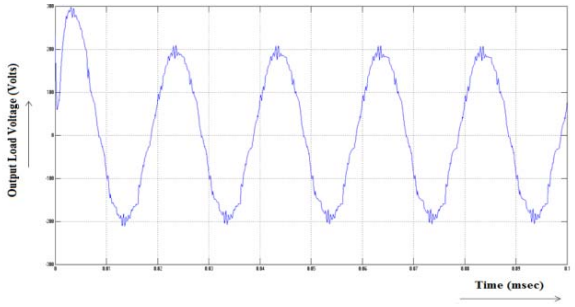

Figure-11. Load voltage waveform of closed loop seven level FCMLI system.

Experimental setup of closed loop seven level FCMLI system

Figure-12.Shows the photographic view of HARDWARE laboratory module with a single phase induction motor load.

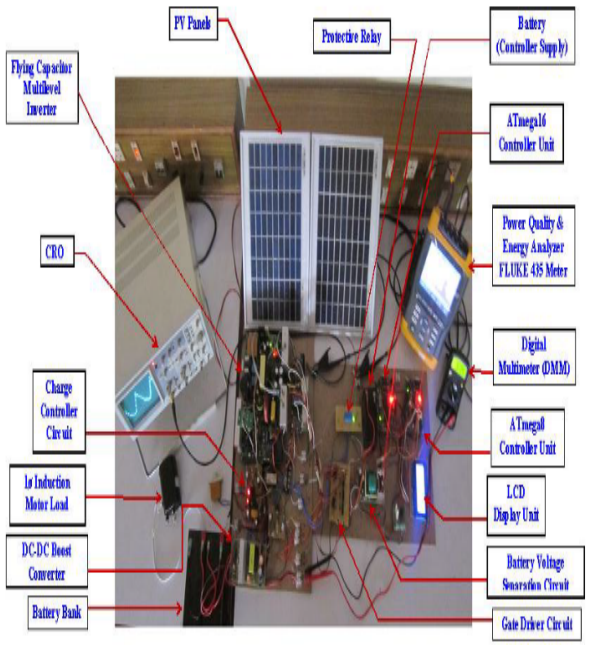

Figure-12. Photographic view of hardware laboratory module with single phase induction motor load.

Hardware results and discussion

The input supply to the proposed system is about 24V DC which is obtained from the two numbers of serially connected 12V, 10W, 1A PV panels. The charge controller circuit is used in-between PV panels and battery bank. The main significance of this circuit is to protect the battery from lower charging and over charging problem. Here this circuit is used to produce the constant DC voltage of 24V DC, which is needed to charge the 24V DC

battery bank. The 24V DC output voltage from the Charge Controller circuit is given to the 24V DC capacity battery bank. From the battery bank, a constant voltage of 24V DC is obtained and which is given to the boost converter circuit for further process. In Figures 13, 14 and 15 show the DC output voltage waveforms of a PV panel, charge controller and charge controller respectively.

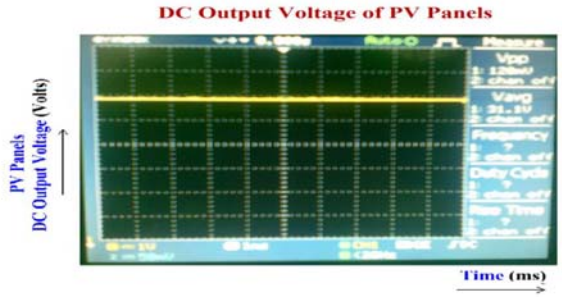

Figure-13. DC output voltage waveform of a PV panel.

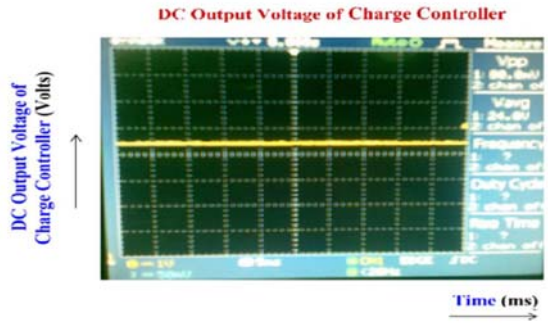

Figure-14. DC output voltage waveform of charge controller.

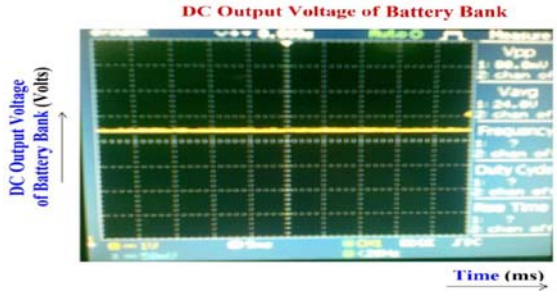

Figure-15. DC output voltage waveform of a battery bank.

Figures 16 and 17 show the switching pulse waveform and DC output voltage waveforms of boost converter.

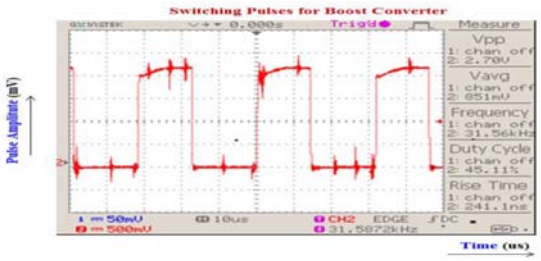

Figure-16. Switching pulse waveform for boost converter.

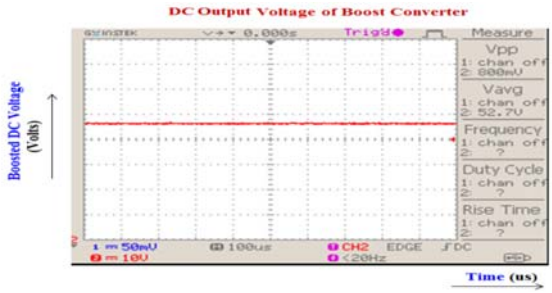

Figure-17. DC output voltage waveform of boost converter.

The PWM control signal for the MOSFET's - IRF540 used in the boost converter circuit is generated from PB1 (Pin 15) of ATmega8 microcontroller. This control signal is then given to the gate driver IC KA3525A, which produces the switching pulses in order to switch the MOSFET switches at f_s = 31.5kHz.The width of the pulse waveform will vary depending upon the output voltage requirement. In boost converter circuit, when the MOSFET's - IRF540 are switched at the switching frequency fs of 31.5 kHz with the help of gate driver KA3525A a boosted voltage of 48V DC is obtained at the output of boost converter.

Figure-18 shows the AC stepped output voltage waveform of closed loop seven level FCMLI. From Figure-19, it is clear that the level of THD is about 4.7% and it is observed that its value lies within 5% as per the standard of International Electro-technical Commission (IEC). Figures 20 and 21 show the AC load voltage waveform and FFT spectrum of closed loop seven level FCMLI system with an incandescent lamp load. Figure-22 shows the AC load voltage waveform and FFT spectrum of closed loop seven level FCMLI system with a single phase induction motor load.

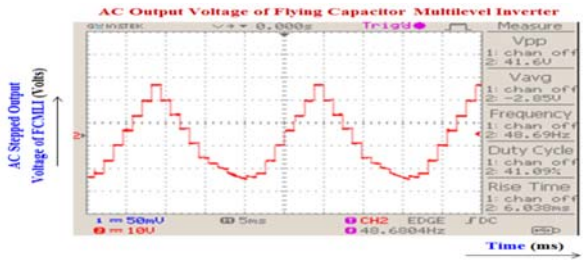

Figure-18. AC stepped output voltage waveform of closed loop seven level FCMLI.

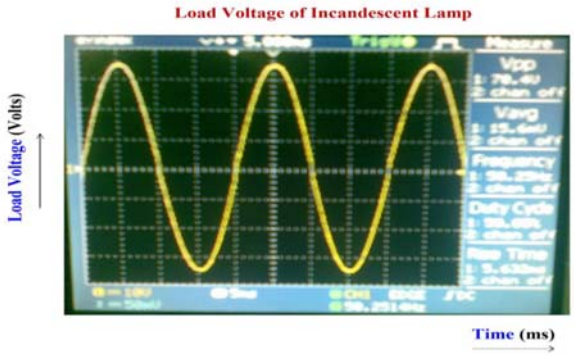

Figure-19. AC load voltage waveform of closed loop seven Level FCMLI system with incandescent lamp load

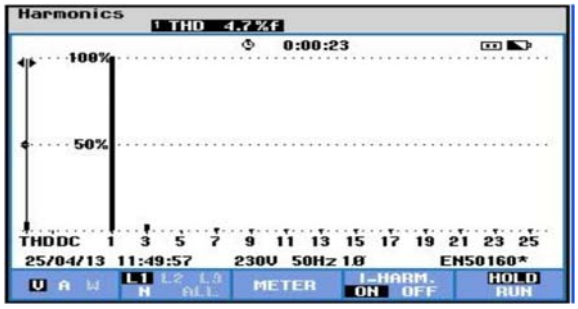

Figure-20. FFT spectrum of closed loop seven level FCMLI system with incandescent lamp load.

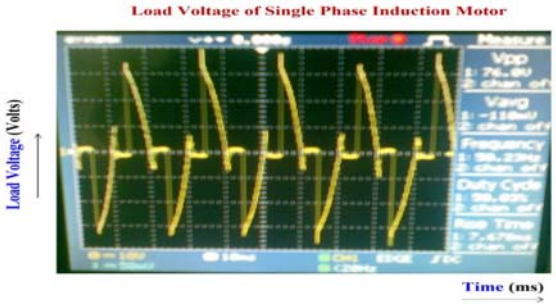

Figure-21. AC load voltage waveform of closed loop seven level FCMLI system with single phase induction motor load.

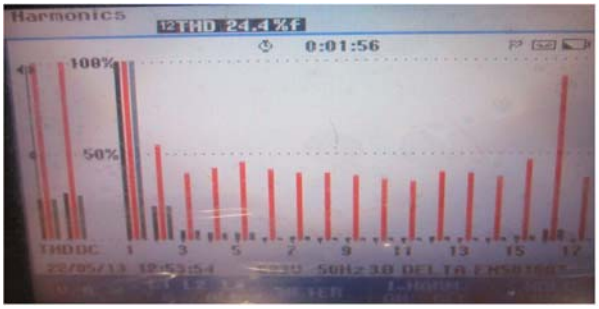

Figure-22. FFT spectrum of closed loop seven level FCMLI system with single phase induction motor load.

From Figure-22, it is observed that the level of THD is higher than the incandescent lamp load. This is due to the non-linear property of induction motor. The Table-3 shows the overall output results of the proposed system.

Table-3. Overall results of proposed system.

Case No.	Working platform	Control scheme	Performance analysis	Connected load	THD level
A	Simulation Tool	Open Loop	FFT Analysis of Seven level FCMLI	R Load	37.15%
B	Simulation Tool	Closed Loop	FFT Analysis of Seven level FCMLI	R Load	10.18%
C	Hardware Module	Closed Loop	FFT Analysis of Seven level FCMLI	Single Phase Induction Motor	24.4%
D	Hardware Module	Closed Loop	FFT Analysis of Seven level FCMLI	Incandescent Lamp	4.7%

CONCLUSIONS

The performance of the developed system was improved through simulation models by using MATLAB software and it was experimentally verified through HARDWARE laboratory module.

From the simulation study, the important conclusions are,

From the output of Stand-alone single PV panel, a unidirectional DC voltage of 12V was produced based on the panel parameters and insolation level.

From the output of capacitor clamped DC/DC boost converter, a boosted DC voltage of 48V DC is produced with the help of single switching device thereby switching loss and circuit complexity are reduced.

From the output of FCMLI, an AC output voltage of 48V AC stepped signals is obtained. There by THD level is reduced when compared to conventional full bridge / half bridge inverters.

From the proposed system, stable operation can be ensured without more disturbances.

REFERENCES

[1] R-J Wai, W-H Wang, C-Y Lin. High-Performance Stand-Alone Photovoltaic Generation System. IEEE Trans. Ind. Electron, 55(1): 240-250.

[2] P.V. Thakre S. Rangnekar.Simulation and Hardware Implementation of MPPT based Single Phase Photovoltaic Inverter using TMS320C28027 Control. International Journal of Computer and Electrical Engineering, 3(4): 592-596.

[3] J.M. Carrasco, LG. Franquelo, J.T. Bialasiewicz,E. Galvan,R.C.P. Guisado, M.A.M. Prats, J.I. Leon, N. Moreno-Alfonso. Power-electronic Systems for the Grid Integration of Renewable Energy Sources: A Survey. IEEE Trans. Ind. Electron, 53(4): 1002–1016.

[4] F. Blaabjerg, Z. Chen, S.B. Kjaer. Power Electronics as Efficient Interface in Dispersed Power Generation Systems. IEEE Trans. Power Electron, 19(5): 1184–1194.

[5] E. Roman, R. Alonso, P. Ibanez, S. Elorduizapatarietxe, D. Goitia. Intelligent PV Module for Grid-connected PV Systems. IEEE Trans. Ind. Electron, 53(4): 1066-1073.

[6] Wai R.J, Wang W.H, Lin C.Y.High Performance Stand-alone Photovoltaic Generation System. IEEE Trans. Ind. Electron, 55(1): 240-250.

[7] Dave Freeman. Introduction to Photovoltaic Systems Maximum Power Point Tracking.Texas Instruments, Application Report, SLVA446.

[8] R.R. Aparnathi, V.V Dwivedi. Design and Simulation Low Voltage Single-Phase Transformerless Photovoltaic Inverter. TELKOMNIKA Indonesian Journal of Electrical Engineering, 12(7): 5163-5173.

[9] M. Irwanto, M.R. Mamat, N. Gomesh, Y.M Irwan. Effect of Maximum Voltage Angle on Three-Level Single Phase Transformerless Photovoltaic Inverter Performance. TELKOMNIKA Indonesian Journal of Electrical Engineering, 12(8): 5886-5896.

[10] K. Jain, P. Chaturvedi. Matlab - based Simulation and Analysis of Three-level SPWM Inverter. International Journal of Soft Computing and Engineering (IJSCE), 2(1): 56-59.

[11] D.W Kang, B.K. Lee, J.H. Jeon, T.J. Kim, D.S Hyun. Asymmetric Carrier Technique of CRPWM for Voltage Balance Method of Flying Capacitor

Multilevel Inverter. IEEE Trans. Ind. Electronics, 52(3); 879-888.

[12] A.M. Soomro, X. Lingyu, S.F. Khahro, L. Xiaozhong. High Output Voltage based Multiphase Step-Up DC-DC Converter Topology with Voltage Doubler Rectifiers. TELKOMNIKA Indonesian Journal of Electrical Engineering, 11(2): 1063-1068.

[13] J. Bauman, M. Kazerani. A Novel Capacitor-Switched Regenerative Snubber for DC/DC Boost Converters. IEEE Trans. Ind. Electron, 58(2): 514-523.

[14] C. Gupta, D. Kuanr, A. Varshney, T. Khurshaid, K. D. Singh, Harmonic Analysis of Seven and Nine Level Cascade Multilevel Inverter using Multi-Carrier PWM Technique, International Journal of Power Electronics and Drive System (IJPEDS),5(1):76-82.

[15] J. Huang, K. Corzine. An Extended Operation of Flying Capacitor Multilevel Inverters. IEEE Trans. Power. Electron, 21(1): 140-147.

[16] R. Kannan, A. Krishnan. High Performance Flying Capacitor based Multilevel Inverter fed Induction Motor. International Journal of Recent Trends in Engineering, 2(2): 7-9.

[17] W. Fei, X. Du, B. Wu, A Generalized Half-wave Symmetry SHE-PWM formulation for Multilevel Voltage Inverters, IEEE Trans. Industrial Electron, 57(9):3030–3038.

[18] S. Kouro, J. Rebolledo, J. Rodriguez, Reduced Switching-frequency Modulation Algorithm for High-power Multilevel Inverters, IEEE Trans. Industrial Electron, 54(5): 2894-2901.

[19] R. Kannan and A.Krishnan, Switching Pattern Selection Scheme Based 11 levels Flying Capacitor Multilevel Inverter Fed Induction Motor, European Journal of Scientific Research, 48(1): 51-62.

[20] K Satyanarayana, B Anjaneyulu, K Siva Prasad, Performance Improvement of Multi Level Inverter fed Vector Controlled Induction Motor Drive for Low Speed Operations, International Journal of Power Electronics and Drive System, 4(1): 51-60.

[21] José Rodríguez, Steffen Bernet, BinWu, Jorge O. Pontt, Samir Kouro, Multilevel Voltage-Source-Converter Topologies for Industrial Medium-Voltage Drives, IEEE Trans. Ind. Electron, 54(6): 2930-2945.